

# Fluorescent chemosensors for Zn<sup>2+</sup>

Zhaochao Xu,<sup>abc</sup> Juyoung Yoon<sup>\*b</sup> and David R. Spring<sup>\*a</sup>

Received 15th January 2010

First published as an Advance Article on the web 28th April 2010

DOI: 10.1039/b916287a

In the past decade, fluorescent chemosensors for zinc ion (Zn<sup>2+</sup>) have attracted great attention because of the biological significance of zinc combined with the simplicity and high sensitivity of fluorescence assays. Chemosensors can be divided into a fluorophore, a spacer and a receptor unit; the receptor is the central processing unit (CPU) of a chemosensor. This *tutorial review* will classify zinc chemosensors based on receptor types.

## 1. Introduction

Fluorescent chemosensors have been developed to be a useful tool to sense *in vitro* and *in vivo* biologically important species such as metal ions and anions because of the simplicity and high sensitivity of fluorescence assays.<sup>1</sup> A typical fluorescent chemosensor contains a receptor (the recognition site) linked to a fluorophore (the signal source) which translates the recognition event into the fluorescence signal.<sup>2</sup> Therefore, an ideal fluorescent chemosensor must meet two basic requirements: firstly, the receptor must have the strongest affinity with the relevant target (binding-selectivity). Secondly, on the basis of good binding-selectivity, the fluorescence signal should avoid environmental interference (signal-selectivity), such as photobleaching, sensor molecule concentration, the environment around the sensor molecule (pH, polarity, temperature, and so forth), and stability under illumination. According

to the well-known fluorophore–spacer–receptor scaffold, the receptor is the central processing unit (CPU) of a chemosensor. Although the ultimate aim for a fluorescent chemosensor is to image the target of interest in a biological setting, a thorough understanding of the available constructs can help to elucidate and improve the design of chemosensors.

Zinc ion (Zn<sup>2+</sup>) has attracted a great deal of attention ascribing to the biological significance of zinc. Zinc is the second most abundant transition metal ion in the human body after iron. Zn<sup>2+</sup> is now recognized as one of the most important cations in catalytic centers and structural cofactors of many Zn<sup>2+</sup>-containing enzymes and DNA-binding proteins (*e.g.*, transcription factors). Zinc is believed to be an essential factor in many biological processes such as brain function and pathology, gene transcription, immune function, and mammalian reproduction,<sup>3</sup> as well as some pathological processes, such as Alzheimer's disease, epilepsy, ischemic stroke, and infantile diarrhea.<sup>4</sup> Although most Zn<sup>2+</sup> is tightly bound to enzymes and proteins, free zinc pools exist in some tissues such as the brain, intestine, pancreas, and retina. Because Zn<sup>2+</sup> is spectroscopically silent due to its d<sup>10</sup> electron configuration, many fluorescent chemosensors for the detection of Zn<sup>2+</sup> have been studied intensively. Several reviews have focused on various aspects of zinc fluorescent chemosensors,<sup>5–8</sup> like fluorescence signal transduction,<sup>6,7</sup> fluorophores used in zinc

<sup>a</sup> Department of Chemistry, University of Cambridge, Cambridge, CB2 1EW, UK. E-mail: spring@ch.cam.ac.uk;

Fax: +44 (0)1223 336362; Tel: +44 (0)1223 336498

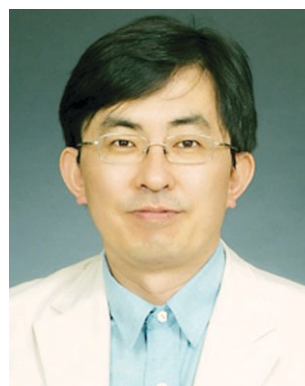
<sup>b</sup> Department of Chemistry and Nano Science (BK21) and Department of Bioinspired Science, Ewha Womans University, Seoul 120-750, Korea. E-mail: jyoony@ewha.ac.kr; Fax: +82-2-3277-2384; Tel: +82-2-3277-2400

<sup>c</sup> State Key Laboratory of Fine Chemicals, Dalian University of Technology, Dalian 116012, China



Zhaochao Xu

Zhaochao Xu was born in Qingdao, China, in 1979. He received his PhD in 2006 from Dalian University of Technology under the supervision of Prof. Xuhong Qian. Subsequently, he joined the group of Juyoung Yoon at Ewha Womans University as a postdoctoral researcher. Since October 2008, he is a Herchel Smith Postdoctoral Research Fellow at University of Cambridge in the group of David R. Spring.



Juyoung Yoon

Juyoung Yoon received his PhD (1994) from The Ohio State University. After completing postdoctoral research at UCLA and at Scripps Research Institute, he joined the faculty at Silla University in 1998. In 2002, he moved to Ewha Womans University, where he is currently a Professor of the Department of Chemistry and Nano Science and Department of Bioinspired Science. His research interests include investigations of fluorescent chemosensors, molecular recognition and organo EL materials.

chemosensors,<sup>8</sup> and the excitation source.<sup>5</sup> This tutorial review will classify zinc chemosensors based on receptor types and help to elucidate the design and application of fluorescent chemosensors for zinc ion in an accessible way to those new to the field.

## 2. Mechanism of Zn<sup>2+</sup> sensing

The signal of a fluorescent chemosensor is usually measured as a change in fluorescence intensity, fluorescence lifetime, or a shift of fluorescence wavelength. The most applied mechanisms of fluorescence signal transduction in the design of Zn<sup>2+</sup> chemosensors are photoinduced electron transfer (PET) and intermolecular charge transfer (ICT) which have been well reviewed by de Silva *et al.*<sup>2</sup> However, the basic concepts of these two mechanisms are explained below.

For a PET chemosensor, a fluorophore is usually connected *via* a spacer to a receptor containing a relatively high-energy non-bonding electron pair, such as nitrogen atom, which can transfer an electron to the excited fluorophore and as a result quench the fluorescence. When this electron pair is bound by coordination of a cation, the redox potential of the receptor is raised so that the HOMO of the receptor becomes lower in energy than that of the fluorophore. Thus, the PET process from the receptor to the fluorophore is blocked and the fluorescence is switched on. A spacer module holds the fluorophore and receptor close to, but separated from, each other. Generally, the best spacer length between the fluorophore and receptor is less than a three-carbon linker, which can guarantee the maximum efficiency for PET. Most of the PET type chemosensors sense Zn<sup>2+</sup> with a fluorescence enhancement signal. However, ratiometric measurements, *i.e.* the observation of changes in the ratio of the intensity of the absorption or the emission at two wavelengths, would be more favorable to increase the signal-selectivity. The ICT mechanism has been widely used in the design of *ratiometric* fluorescent chemosensors. When a fluorophore, without a spacer, is directly connected to a receptor (usually an amino group) to form a  $\pi$ -electron conjugation system with electron rich and

electron poor terminals, then ICT from the electron donor to receptor would be enhanced upon excitation by light. When a receptor (playing the role of an electron donor within the fluorophore) interacts with a cation, it reduces the electron-donating character of the receptor and a blue shift of the emission spectrum is expected. In the same way, if a cation receptor plays the role of an electron receptor, the interaction between the receptor and the cation would further strengthen the push-pull effects. Then a red shift in emission would be observed. For example, the coordination of Zn<sup>2+</sup> by quinoline derivatives can induce a red-shifted ratiometric fluorescence signal.

It is worth mentioning that the combination of PET and ICT mechanisms in the design of chemosensors would be valuable, since a wavelength-shifted fluorescence intensity enhancement will amplify the recognition event to a greater extent.

## 3. Di-2-picolylamine (DPA) as the receptor

After the first incorporation to fluorescein in 1996,<sup>9</sup> di-2-picolylamine (DPA) has been used as the most popular receptor to construct Zn<sup>2+</sup> chemosensors. DPA is a derivative of *N,N,N',N'*-tetrakis(2-pyridylmethyl)-ethylenediamine (TPEN, Fig. 1) which is a classical membrane-permeable Zn<sup>2+</sup> chelator with high selectivity for Zn<sup>2+</sup> over alkali and alkaline-earth metal ions that occur in much higher concentrations in biological samples, such as Ca<sup>2+</sup>, Mg<sup>2+</sup>, K<sup>+</sup>, Na<sup>+</sup>.

### 3.1 DPA

The straightforward way to construct DPA based chemosensors is to directly connect DPA to various fluorophores. The secondary amine nitrogen atom of DPA serves as a good reaction site to be linked to various fluorophores and an effective signal transduction sponsor to respond to the binding events through PET or ICT mechanisms. Compound **1** is a typical PET chemosensor for proton and post-transition metal ions like Zn<sup>2+</sup> with DPA conjugated to anthracene.<sup>10</sup> The methylene group allows a PET process from the aliphatic amine nitrogen of DPA to the excited anthracene which quenches the fluorescence. Upon binding of Zn<sup>2+</sup>, the PET process is prevented, which resulted in a significant enhancement of fluorescence.

However, effective fluorescent chemosensors for Zn<sup>2+</sup> in living systems must meet several requirements,<sup>5</sup> such as high selectivity and sensitivity toward Zn<sup>2+</sup>, visible or near-infrared (NIR) excitation and emission profiles to avoid cell damage, large extinction coefficients and quantum yields, turn-on increase or a ratiometric response to Zn<sup>2+</sup>, and so on. Fluorescein derivative **2** reported by the Lippard group has



David R. Spring

David Spring gained his DPhil for work on the proposed biosynthesis of the manzamine alkaloids at Oxford University under the supervision of Professor Sir Jack E. Baldwin FRS. Later he spent two and a half years as a Wellcome Trust Postdoctoral Fellow and Fulbright Scholar at Harvard University with Professor Stuart L. Schreiber. He is currently an EPSRC Advanced Fellow at the University of Cambridge, Chemistry Department. David's research programme is focused on the use of chemistry to explore biology.

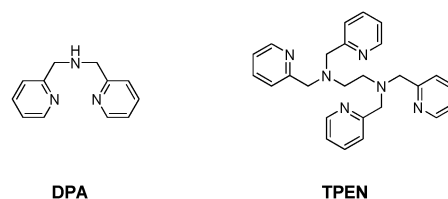


Fig. 1 Structures of DPA and TPEN.

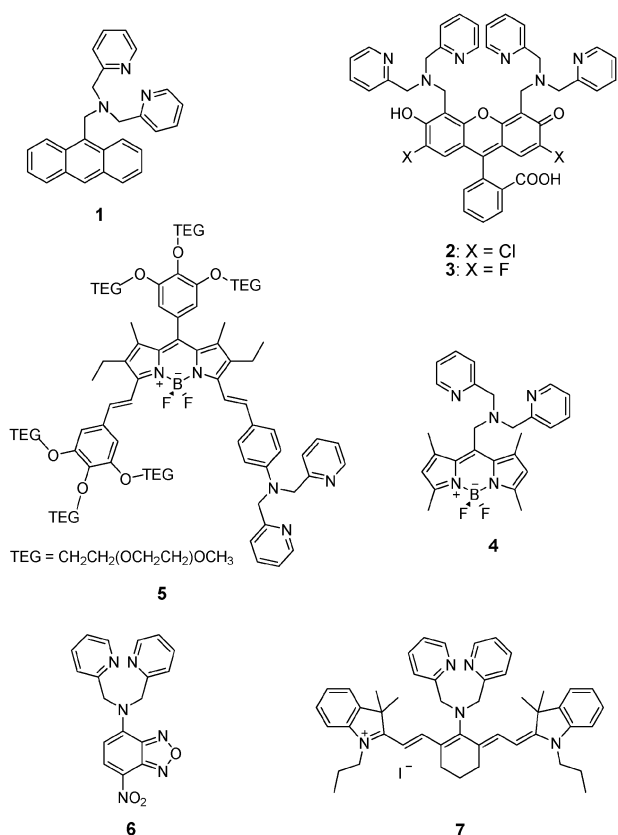


Fig. 2 Structures of chemosensors 1–7 with DPA as receptor.

the advantages of absorption in the visible region and a high quantum yield of fluorescence in aqueous solutions (Fig. 2).<sup>11</sup> Compound **2** shows a selective fluorescence enhancement (2.2 fold) with Zn<sup>2+</sup> over Ca<sup>2+</sup> and Mg<sup>2+</sup> that are abundant in cellular systems. But a problem confining fluorescein derivatives is their pH-sensitivity around neutral conditions that will interfere with the Zn<sup>2+</sup> binding signal. The introduction of electron-withdrawing fluorine atoms into the fluorescein scaffold (**3**)<sup>12</sup> reduced the pK<sub>a</sub> to 6.8 in contrast with the pK<sub>a</sub> value of 8.4 for **2**.

Bodipy dyes are relatively insensitive to the polarity and pH of their environment and are reasonably stable to physiological conditions with narrow emission bandwidths and high quantum yields.<sup>13</sup> The PET chemosensor **4**<sup>14</sup> reported by the Peng group that derived from the bodipy fluorophore exhibited a selective fluorescence enhancement (7 fold) upon Zn<sup>2+</sup> binding with a low pK<sub>a</sub> value (2.1), low dissociation constant ( $K_d = 1.0$  nM) and high quantum yield of the zinc-bound species ( $\Phi_F = 0.857$ ) (Fig. 2). A water soluble distyryl-bodipy dye **5**<sup>15</sup> was reported recently by Akkaya *et al.* for Zn<sup>2+</sup> sensing. Beside water solubility, another favorable feature of **5** is the emission wavelength shift in NIR region from 730 nm to 680 nm on Zn<sup>2+</sup> ion binding with the potential of a ratiometric assay (Fig. 2). The interaction between the amine nitrogen of DPA and Zn<sup>2+</sup> blue-shifted both the absorption and fluorescence spectra of **5** based on the ICT mechanism. The aromatic amine nitrogen of DPA conjugated to the fluorophore reduces the pK<sub>a</sub> value, processes the signal transduction through an ICT mechanism, and simultaneously

decreases the zinc affinity owing to its electron-donating ability to the fluorophore, which acts as an electron acceptor. For example, the dissociation constant of **5** with zinc was reported as 20  $\mu$ M, much less than that of **4**. In contrast, no fluorescence alteration for compound **6**<sup>16</sup> was observed with the addition of Zn<sup>2+</sup> indicating the relatively low affinity of DPA in **6** for Zn<sup>2+</sup>, possibly due to the strong electron-withdrawing ability of the 7-nitrobenz-2-oxa-1,3-diazole (NBD) fluorophore.

NIR fluorescent sensors are of great interest for potential *in vivo* imaging applications.<sup>17</sup> In the near-infrared region biological samples have low background fluorescence signals, providing a high signal to noise ratio. Meanwhile, near-infrared radiation can penetrate into sample matrices deeply due to low light scattering. A NIR chemosensor **7**<sup>18</sup> reported by Tang *et al.* contains the DPA receptor connected with a propyl-substituted tricyanin fluorophore and gave a 20-fold turn-on fluorescence response with the emission at 780 nm for detecting Zn<sup>2+</sup> (Fig. 2).

### 3.2 DPA derivatives

In order to improve the zinc affinity, fast zinc complex formation rate and high zinc complex stability, some DPA-derivatives with fourth and/or fifth additional coordination sites, such as *N,N*-di-(2-picolyl)ethylenediamine (DPEN) and *N,N,N'*-tris(pyridin-2-ylmethyl)ethylenediamine (TRPEN), were applied to construct fluorescent chemosensors. Nagano *et al.* designed ligands **8** (DPEN structure) and **9** (TRPEN structure) for high Zn<sup>2+</sup> selectivity and a sulfonic acid moiety for hydrophilicity (Fig. 3).<sup>19</sup> The dissociation constants of **8** and **9** with zinc were reported as 1.6 pM and 0.5 pM, respectively. Compounds **8** and **9** also show very rapid chelation rates for Zn<sup>2+</sup> which are comparable to that of TPEN. DPEN was firstly introduced into the fluorescein scaffold by Nagano *et al.* to make the PET chemosensors **10** and **11** with large turn-on responses (17-fold for **10** and 51-fold for **11**) and high Zn<sup>2+</sup> affinity (0.78 nM for **10** and 2.7 nM for **11**).<sup>20</sup> Possibly due to the strong electron-withdrawing nature of the carboxylic acid group, Zn<sup>2+</sup> cannot interact with the aniline, therefore there were no changes both in excitation and emission maxima of **10** and **11** with addition of Zn<sup>2+</sup>. In subsequent work,<sup>21</sup> the Nagano group changed the fluorophore to benzofuran to make chemosensors **12** and **13**. The aniline nitrogens of **12** and **13** have a higher basicity than those of **10** and **11**, therefore they coordinate with Zn<sup>2+</sup> resulting in a blue shift in the absorption and excitation maxima based on the ICT mechanism, whereas the emission maxima were less affected due to cation ejection during the excited state. The Nagano group also reported a ratiometric NIR chemosensor (**14**) for Zn<sup>2+</sup> connecting the DPEN receptor with a tricyanin fluorophore.<sup>22</sup> With the addition of Zn<sup>2+</sup> ( $K_d = 98$  nM), a 44 nm red shift of the absorption maximum was observed. Accordingly, the maximum of the excitation wavelength shifted from 627 nm to 671 nm with an increase in intensity.

The 4-amino-1,8-naphthalimide was also introduced as a fluorophore in the design of DPEN-based chemosensors. In chemosensor **15** (Fig. 3) reported by the Qian group,<sup>23</sup> the receptor DPEN was attached to the fluorophore through a

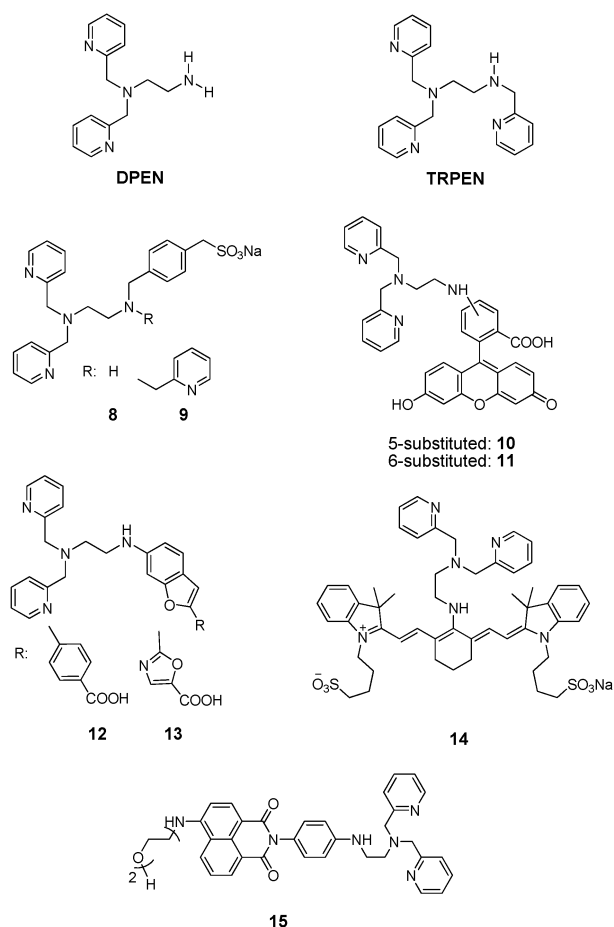


Fig. 3 Structures of chemosensors 8–15 with DPEN as receptor.

benzene ring on the imide moiety using the virtually decoupled fluorophore–receptor linking strategy. The lone pair electron of the aniline nitrogen quenches the fluorescence of the excited fluorophore 4-aminonaphthalimide by the PET mechanism. When the electron-donating aniline nitrogen is complexed with  $\text{Zn}^{2+}$ , the PET process is blocked to get a 6-fold increase in emission. The apparent dissociation constant of **15** was 0.62 nM.

Xu *et al.* incorporated TRPEN with *N*-substituted-4-bromo-5-nitro-1,8-naphthalimide to develop a ratiometric chemosensor **16** for  $\text{Zn}^{2+}$  (Fig. 4).<sup>24</sup> The capture of  $\text{Zn}^{2+}$  by the receptor resulted in the deprotonation of the secondary amine conjugated to 1,8-naphthalimide so that the electron-donating ability of the N atom would be greatly enhanced; thus **16** showed a 56 nm red-shift in absorption (507 nm) and fluorescence spectra (593 nm,  $\Phi_F = 0.14$ ), respectively, from which

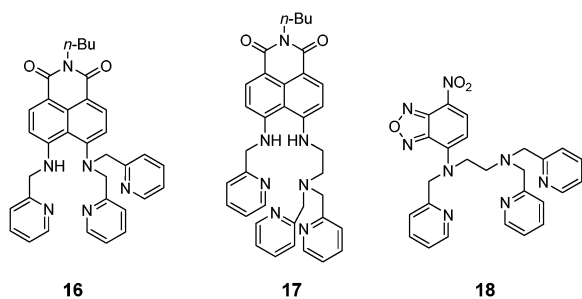


Fig. 4 Structures of chemosensors 16–18 with TRPEN as receptor.

one could sense  $\text{Zn}^{2+}$  ratiometrically and colorimetrically. Xu *et al.* then extended the  $\text{Zn}^{2+}$ -deprotonation mechanism to construct chemosensor **17** which can discriminate  $\text{Zn}^{2+}$  and  $\text{Cd}^{2+}$  by undergoing different ICT processes.<sup>25</sup>  $\text{Cd}^{2+}$  binding induces a blue shift in emission from 531 nm to 487 nm based on a general ICT mechanism, while  $\text{Zn}^{2+}$  binding produces a red shift in emission from 531 nm to 558 nm through the deprotonation–ICT mechanism. An NBD based TRPEN chemosensor **18** was also reported recently.<sup>26,27</sup> Compound **18** displayed a red-to-yellow color change and a selective enhancement of fluorescent intensity in the presence of  $\text{Zn}^{2+}$  in water with a slight wavelength change. A combination of PET and ICT mechanisms are responsible for these changes.

From the above discussion, the ICT mechanism has been proved to be a rational strategy to design ratiometric chemosensors for  $\text{Zn}^{2+}$ . For those nitrogen-containing heterocyclic chromophores whose nitrogen can complex metal ions, like pyridine and benzimidazole derivatives,  $\text{Zn}^{2+}$  binding can induce large wavelength shifts in emission in contrast with **12–14**. Particularly, if the heterocyclic component operates as an electron-withdrawing group, the coordination of a hetero atom with  $\text{Zn}^{2+}$  will red-shift the emission. Guo *et al.* reported **19** as a ratiometric chemosensor for  $\text{Zn}^{2+}$  based on the 2-(2'-pyridinyl)benzimidazole (2-PBI) ionophore incorporating the DPA receptor which showed strong binding affinity ( $K_d = 7.9$  pM) (Fig. 5).<sup>28</sup> The  $\text{Zn}^{2+}$ -induced red emission shift (63 nm) of **19** could be correlated to the coplanation of two heteroaromatic planes of 2-PBI via  $\text{Zn}^{2+}$ -induced reversion or rotation. Compound **20** is a ratiometric  $\text{Zn}^{2+}$  sensor reported by the O'Halloran group, which combined a benzoxazole reporter with an appended phenolic group and a picolyl amine group for tight  $\text{Zn}^{2+}$  binding ( $K_d = 2.2$  nM) and high  $\text{Zn}^{2+}$  selectivity.<sup>29</sup>  $\text{Zn}^{2+}$  binding produced red shifts in excitation (from 337 nm to 376 nm) and emission (from 407 nm to 443 nm) wavelengths. An iminocoumarin-based chemosensor **21** was recently reported with a high quantum yield in aqueous media on excitation in the visible wavelength region.<sup>30</sup> **21** is selective for  $\text{Zn}^{2+}$  over other biologically important metal ions, such as  $\text{Ca}^{2+}$  and  $\text{Mg}^{2+}$ , and has high affinity for  $\text{Zn}^{2+}$  ( $K_d = 1.3$  pM). Compound **21** was confirmed to be directly applicable to monitor changes in intracellular  $\text{Zn}^{2+}$  ratiometrically in cultured cells and in rat hippocampal slices.

### 3.3 Amide-DPA receptor based on $\text{Zn}^{2+}$ -triggered amide tautomerization

Even though DPA-based receptors have higher affinities for  $\text{Zn}^{2+}$  over alkali and alkaline-earth metal ions, they show similar affinities for most of transition and heavy metal (HTM)

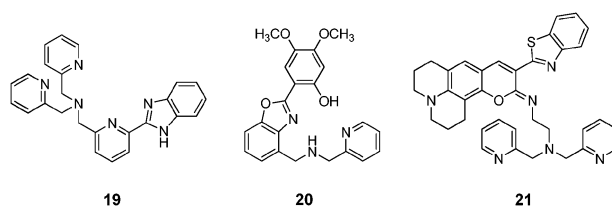


Fig. 5 Structures of chemosensors 19–21.

ions. That means even though DPA chemosensors show a selective turn-on or ratiometric fluorescence signal for  $\text{Zn}^{2+}$ , they often display poor binding selectivity for  $\text{Zn}^{2+}$  over other HTM ions. Recently, Xu *et al.* reported an amide-containing DPA receptor for  $\text{Zn}^{2+}$ , combined with a naphthalimide fluorophore (**22**, Fig. 6).<sup>31</sup> Compound **22** binds  $\text{Zn}^{2+}$  in an imidic acid tautomeric form of the amide-DPA receptor in aqueous solutions with the highest affinity ( $K_d = 5.7$  nM), while most other HTM ions are bound to the chemosensor in an amide tautomeric form (Fig. 6). This strategy can be called 'receptor transformation'. Due to this differential binding mode, **22** showed excellent selectivity for  $\text{Zn}^{2+}$  over most competitive HTM ions with an enhanced fluorescence (22 fold) as well as a red-shift in emission from 483 nm to 514 nm. Interestingly, the **22**/ $\text{Cd}^{2+}$  complex ( $K_d = 48.5$  nM) showed an enhanced (21 fold) blue-shift in emission from 483 nm to 446 nm. Therefore, **22** could discriminate *in vitro* and *in vivo*  $\text{Zn}^{2+}$  and  $\text{Cd}^{2+}$  with green and blue fluorescence, respectively (Fig. 7). Due to the stronger affinity,  $\text{Zn}^{2+}$  could be ratiometrically detected *in vitro* and *in vivo* with a large emission wavelength shift from 446 nm to 514 nm *via* a  $\text{Cd}^{2+}$  displacement approach. **22** was also successfully used to image intracellular  $\text{Zn}^{2+}$  ions in the presence of iron ions. Finally, **22** was successfully applied to detect zinc ions during the development of living zebrafish embryos (Fig. 8).

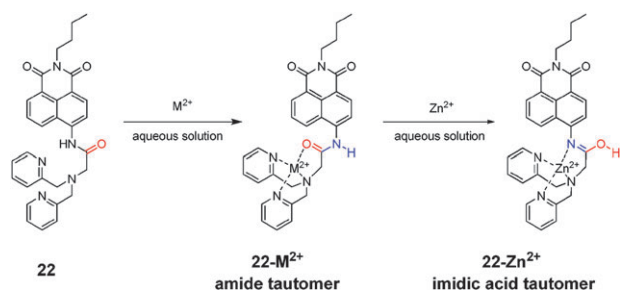


Fig. 6 Different binding modes of **22** with HTM ions.

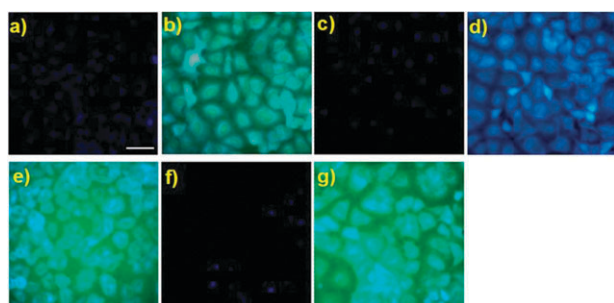


Fig. 7 Fluorescence images of A549 cells incubated with  $5 \mu\text{M}$  **22** and ions. (a) Images of cells treated with **22** in the absence and (b) presence of  $1 \mu\text{M}$  of external zinc ions, and (c) image of cells after treatment with **22** and  $1 \mu\text{M}$   $\text{ZnCl}_2$  and subsequent treatment of the cells with  $25 \mu\text{M}$  TPEN. (d) Images of cells treated with **22** in the presence of  $5 \mu\text{M}$   $\text{CdCl}_2$  and (e) image of cells after treatment with **22** and  $5 \mu\text{M}$   $\text{CdCl}_2$  and subsequent treatment of the cells with  $1 \mu\text{M}$   $\text{ZnCl}_2$ . (f) Images of cells treated with **22** in the presence of  $5 \mu\text{M}$   $\text{Fe}(\text{ClO}_4)_2$  and (g) image of cells after treatment with **22** and  $5 \mu\text{M}$   $\text{Fe}(\text{ClO}_4)_2$  and subsequent treatment of the cells with  $1 \mu\text{M}$   $\text{ZnCl}_2$  (bar =  $50 \mu\text{m}$ ).

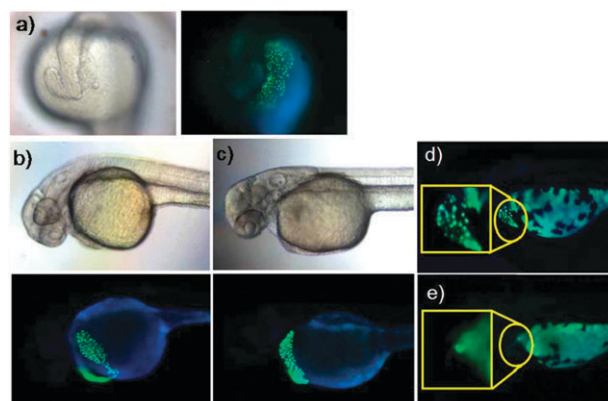


Fig. 8 Zebrafish incubated with  $5 \mu\text{M}$  **22**. (a) Images of 19 h-old, (b) 36 h-old, and (c) 48 h-old zebrafish incubated with **22** for 1 h. (d) Image of 54 h-old zebrafish incubated with **22** for 1 h and (e) image of 54 h-old zebrafish after initial incubation with  $100 \mu\text{M}$  TPEN for 1 h and subsequent treatment of washed zebrafish with **22** for 1 h.

The big advantages of DPA receptors are their fast  $\text{Zn}^{2+}$  chelation, high bio-compatibility and high selectivity for  $\text{Zn}^{2+}$  over alkali and alkaline-earth metal ions. DPA is a commercially available product and can be conveniently connected to various fluorophores. By adding extra binding sites or modifying the DPA moiety, for example, substitution of a DPA pyridine donor with a thiophene donor<sup>32</sup> or increasing the length of one pyridine ligand,<sup>33</sup> the disassociation constants ( $K_d$ ) of DPA receptors can cover the range of  $10^{-12}$ – $10^{-4}$  M, which can fulfill the requirements of various biological  $\text{Zn}^{2+}$  concentrations. One of the disadvantages of DPA receptors is the possible protonation of the aliphatic amine of DPA at  $\text{pH} \approx 6$ , even most of the DPA receptors remain intact at physiological pH. Constructing DPA in ICT sensors can avoid this problem, but the binding affinity and photophysical properties would change dramatically. Another concern is the sightlessness of the DPA receptor for HTM ions. The work of Xu *et al.*<sup>31</sup> about the 'receptor transformation' strategy may elucidate a way to create an artificial receptor for some HTM ions with extreme selectivity.

#### 4. Quinoline as the receptor

Quinoline and its derivatives, particularly 8-hydroxyquinoline and 8-aminoquinoline, are well-known fluorogenic chelators for transition metal ions. An aryl sulfonamide derivative of 8-aminoquinoline **23** (TSQ) is the first and most widely used fluorescent chemosensor for imaging  $\text{Zn}^{2+}$  in biological samples (Fig. 9). It was first introduced by Russian biochemists Toroptsev and Eshchenko in the early 1970s. The popularity of **23** as a physiological stain arose after pioneering work by Frederickson *et al.* in 1987.<sup>34</sup> Chemosensor **23** showed a 100-fold increase in fluorescence with a maximum at 495 nm upon formation of the TSQ–Zn complex and it is membrane-permeable. Compound **23** is the first chemosensor that was selective enough to measure  $\text{Zn}^{2+}$  in the presence of high concentrations of  $\text{Ca}^{2+}$  and  $\text{Mg}^{2+}$ . However, **23** has a poor water-solubility and was found to partition in the cell membrane as well. The stoichiometry of zinc binding is not

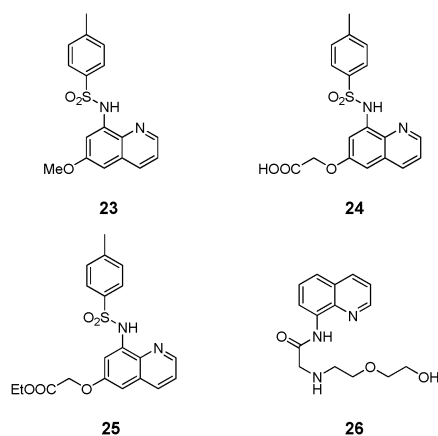


Fig. 9 Structures of chemosensors 23–26.

unequivocal, complicating the ability to quantitatively measure free zinc in cells. To improve the water solubility and membrane permeability, a carboxylic acid or an ester group was introduced into TSQ instead of the 6-methoxy group to produce chemosensor **24** (Zinquin A) and **25** (Zinquin E).<sup>35</sup> Both **24** and **25** showed a large increase in fluorescence upon addition of  $\text{Zn}^{2+}$ .  $\text{Ca}^{2+}$  and  $\text{Mg}^{2+}$  had little effect on the fluorescence whereas  $\text{Fe}^{2+}$  and  $\text{Cu}^{2+}$  quenched the fluorescence.

Recently, an 8-carboxamidoquinoline derivative **26** was reported as a water-soluble and ratiometric fluorescent chemosensor.<sup>36</sup> After binding  $\text{Zn}^{2+}$ , the carboxamido group is deprotonated, and then the intramolecular hydrogen bond of 8-aminoquinoline is broken to inhibit the intramolecular electron-transfer process which quenches quinoline's fluorescence. The introduction of a 2-(2-hydroxyethoxy)-ethylamino group provides not only another two metal coordination sites (carboxamidoquinoline affords two sites) but also a hydrophilic group. Along with the complexation of  $\text{Zn}^{2+}$  by quinoline nitrogen, **26** showed an 8-fold increase in fluorescence quantum yield and a 75 nm red-shift of fluorescence emission upon binding  $\text{Zn}^{2+}$  in buffer aqueous solution.

Quinoline shows moderate zinc affinity ( $K_d = \sim 10^{-6}$  M). With the extra binding sites, the binding constant of quinoline receptors will increase remarkably. For example, to achieve high affinity for zinc ions and water solubility, Jiang *et al.* incorporated DPA into 8-hydroxy-2-methylquinoline at the 2 position and an carboxylic group at the 8 position to get chemosensor **27** (Fig. 10).<sup>37</sup> Compound **27** is water-soluble with a 14-fold enhanced quantum yield upon chelation to zinc ion ( $\lambda_{\text{ex}} = 315$  nm;  $\lambda_{\text{em}} = 435$  nm). NMR studies and the crystal structure of **27**- $\text{Zn}^{2+}$  complex indicate that the

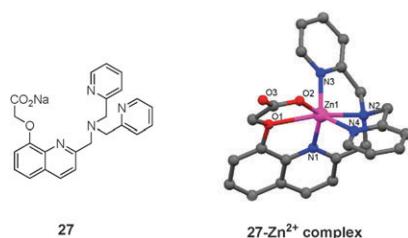


Fig. 10 Structures of chemosensor **27** and its zinc complex.

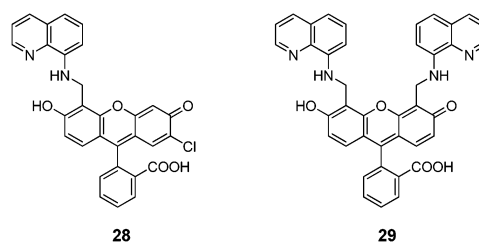


Fig. 11 Structures of chemosensors **28** and **29**.

oxygens at the 8 position (O1) and the carboxylic group (O2) participate in the chelation of the zinc ion along with the quinoline nitrogen atom (N1) and DPA (N2–N4) to endow **27** with a high binding affinity ( $K_d = 0.45$  pM). **27** also exhibited high selectivity to zinc ion even in the presence of some transition metal ions like  $\text{Co}^{2+}$ ,  $\text{Fe}^{2+}$ ,  $\text{Ni}^{2+}$  and  $\text{Cu}^{2+}$ .

Although quinoline moieties can serve as both the metal binding site and the fluorophore, the application of quinoline-based chemosensors in biological systems is limited by their optical properties. The main disadvantage of these chemosensors is high-energy UV excitation, which is potentially damaging to biological tissues and can induce autofluorescence from endogenous components, and fluorescence at short wavelengths ( $\sim 490$  nm). Chemosensors **28** and **29** developed by the Lippard group contain fluorescein as the fluorophore and quinoline as the receptor, and can overcome these shortcomings (Fig. 11).<sup>38</sup> Because of their low background fluorescence and highly emissive  $\text{Zn}^{2+}$  complexes, **28** and **29** show 42 and 150-fold fluorescence enhancements upto  $\text{Zn}^{2+}$  coordination, respectively. **28** and **29** are cell-permeable with micromolar affinity for  $\text{Zn}^{2+}$  (for **28**,  $K_d = 33$   $\mu\text{M}$ ; for **29**,  $K_d = 41$   $\mu\text{M}$ ) which endow **28** and **29** with the value of detecting higher concentrations of intracellular  $\text{Zn}^{2+}$  than most of the DPA-based chemosensors.

## 5. Bipyridine as the receptor

Binding-induced conformational restriction of biaryl fluorophores can efficiently increase the fluorescence intensity.<sup>39</sup> For heterobiaryl fluorophores (*e.g.*, bipyridyl), the coordination of metal ions, through the combination of two signaling mechanisms, that is conformational restriction and intramolecular charge transfer, will produce an enhanced red-shift in fluorescence emission.<sup>40</sup> For example, a bipyridyl moiety was incorporated into a pyrrole-end-capped divinyl aromatic system, which are known to be strongly fluorescent building blocks for the synthesis of electrochromic and low band polymers, to get compound **30** (Fig. 12).<sup>41</sup> Chemosensor **30** fluoresces at 547 nm in aqueous acetonitrile (1 : 9) solution. With the titration of various metal ions, the binding of  $\text{Zn}^{2+}$  by **30** results in a highly selective and red-shifted emission at 635 nm. When  $\text{Zn}^{2+}$  was added to a nonfluorescent  $\text{Cu}^{2+}$  complex of **30**, the emission corresponding to the  $\text{Zn}^{2+}$  complex reappeared, which indicates the preferential binding of  $\text{Zn}^{2+}$ . In compound **31**, the bipyridyl binding site is sterically-encumbered by a *m*-terphenyl moiety to enforce the preferential formation of a 1 : 1 metal–ligand complex.<sup>42</sup>

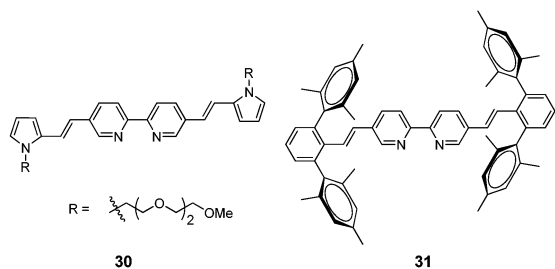


Fig. 12 Structures of chemosensors **30** and **31**.

In response to planarization of the bipyridyl unit, extending the effective conjugation length, in conjunction with the perturbation of the electronic system,  $\text{Zn}^{2+}$  binding of **31** leads to a red shift in absorption (from  $\lambda = 370$  to  $395$  nm) and an enhanced shift in fluorescence emission (21-fold increase, from  $\lambda = 414$  to  $486$  nm).

Recently, the DPA receptor was introduced to the bipyridyl system (Fig. 13, chemosensor **32**).<sup>41</sup> Because of the higher affinity of DPA for  $\text{Zn}^{2+}$  than the bipyridyl moiety, with the addition of  $\text{Zn}^{2+}$ , DPA will bind the first equiv. of  $\text{Zn}^{2+}$  resulting in the fluorescence increase (18 fold) through the PET mechanism, which was followed by the bipyridyl to bind the second equiv. of  $\text{Zn}^{2+}$ , resulting in a bathochromic shift of the emission band (from  $\lambda = 410$  to  $440$  nm) based on the ICT mechanism in a neutral aqueous solution (10 mM HEPES, pH 7.0, 20% DMSO) (Fig. 13). The heteroditopic fluoroionophoric platform of **32** provides a lead structure for constructing fluorescent chemosensors for real-time live cell imaging of zinc ions over broad dynamic ranges. The response range of **32** to total concentration in the aqueous solution was from  $<1 \mu\text{M}$  to  $>1 \text{ mM}$ .<sup>43</sup>

The vinyl-conjugated bipyridine derivatives are another type of fluoroionophore for  $\text{Zn}^{2+}$  with moderate affinity ( $K_{\text{d}} = \sim 10^{-6}$  M). The notable advantage of this type of receptor is the enhanced red-shift in emission induced by  $\text{Zn}^{2+}$  chelation. However, bipyridyl derivatives are the most-employed ligands in coordination chemistry, which stems from their facile preparation/functionalization, stability and ability to bind a wide array of d- and f-block elements. Thus bipyridine receptors usually lack the high selectivity for  $\text{Zn}^{2+}$ . Another drawback is the promiscuity in stoichiometry of bipyridine with various metal ions. In order to get 1 : 1 stoichiometry, bulky groups are positioned at the end of bipyridine.

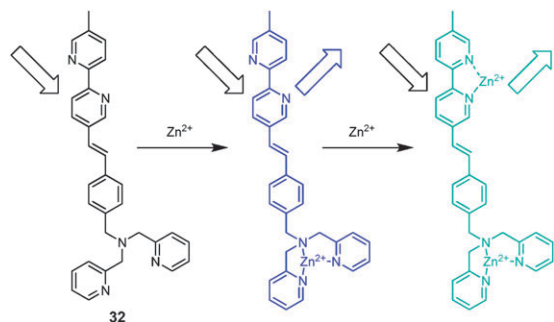


Fig. 13 Photophysical responses of **32** upon coordinating one and two  $\text{Zn}^{2+}$  ions.

## 6. Acyclic and cyclic polyamines as the receptor

To construct fluorescent chemosensors for transition metal ions, the receptor consisting of only one aliphatic amine group is the simplest one undergoing a PET mechanism, which is depending on both the strong affinity of aliphatic amine for transition metal ions and its good electron-donating ability during the PET process. The greatest fluorescence enhancement effect has been usually observed for  $\text{Zn}^{2+}$ , because  $\text{Zn}^{2+}$  has a  $d^{10}$  electronic configuration which does not usually introduce electron- or energy-transfer mechanisms for the deactivation of the excited state. A significant fluorescence quenching can also be observed with some heavy and transition metal ions, such as  $\text{Cr}^{3+}$ ,  $\text{Fe}^{2+}$ ,  $\text{Co}^{2+}$ ,  $\text{Ni}^{2+}$ ,  $\text{Cu}^{2+}$ , and  $\text{Hg}^{2+}$ .<sup>2</sup> To increase the affinity, many examples of chemosensors for transition metal ions are reported whose receptor unit is composed of more than one amine unit. The common disadvantage of polyamines as a  $\text{Zn}^{2+}$  receptor is the lack of binding-selectivity for  $\text{Zn}^{2+}$ .

Czarnik *et al.* reported a 9,10-disubstituted-anthracene derivative **33** (Fig. 14).<sup>44</sup> In **33**, the fluorescence background is very weak due to the efficient quenching of amines. Addition of zinc chloride to acetonitrile solutions of **33** drastically enhances the observed fluorescence intensity over 1000-fold. The same experiments failed in water because of the lower association constant. Anthracene based chemosensors with acyclic polyamine receptors, such as **34** and **35**, were also reported.<sup>45</sup> Compound **35** may be the first ratiometric fluorescent chemosensor for  $\text{Zn}^{2+}$  in aqueous solution. The addition of  $\text{Zn}^{2+}$  induced 4-fold increase in fluorescence intensity at about  $495$  nm ascribed to the anthracene excimer formation. The tripodal ligand **36** containing the dansyl chromophore was reported for post-transition metal sensing.<sup>46</sup> Although this compound shows a remarkable selectivity towards  $\text{Cu}^{2+}$  ions, it forms a 1 : 1 complex upon binding accompanied by a blue-shift and a concomitant 3.7-fold increase of fluorescence quantum yield in basic environments.

Macrocyclic polyamines such as 1,4,7,10-tetraazacyclododecane (cyclen) form very stable  $\text{Zn}^{2+}$  complexes in aqueous solution at neutral pH. Therefore, cyclen is a promising and suitable chelator for  $\text{Zn}^{2+}$  fluorescent chemosensors. Kimura *et al.* reported a dansylamide-pendant cyclen **37** which

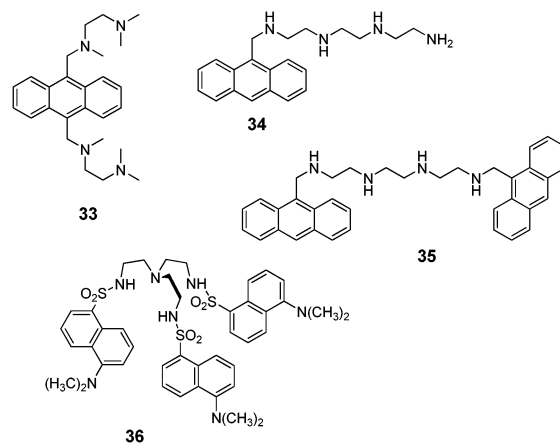


Fig. 14 Structures of chemosensors **33**–**36**.

quantitatively responds to  $\text{Zn}^{2+}$  at submicromolar concentrations in aqueous solution as a result of dansylamide deprotonation.<sup>47</sup> X-Ray crystal analysis reveals that  $\text{Zn}^{2+}$  coordinated to **37** in a distorted square-pyramidal geometry. The dissociation constant ( $K_d$ ) was about 8 pM at pH 7.4. **37** is a stable indicator of apoptosis and acts alone to detect early-stage apoptotic cells.<sup>48</sup> To improve  $\text{Zn}^{2+}$  selectivity and sensitivity, (anthrylmethylamino)ethyl cyclen **38** was reported later by the Kimura group.<sup>49</sup> The emission enhancement in the 1 : 1  $\text{Zn}^{2+}$ –**38** complex is due to the retardation of PET by chelation of a nitrogen atom of the side chain to  $\text{Zn}^{2+}$ . Recently, the Kimura group introduced the 8-hydroxy-5-*N,N*-dimethylaminosulfonyl-quinoline unit to cyclen to make the chemosensor **39**.<sup>50</sup> **39** and  $\text{Zn}^{2+}$  form a 1 : 1 complex, in which the 8-OH group of the quinoline ring is deprotonated and coordinates to  $\text{Zn}^{2+}$  in aqueous solution at neutral pH. On addition of one equivalent of  $\text{Zn}^{2+}$  and  $\text{Cd}^{2+}$ , the fluorescence emission of **39** at 512 nm in 10 mM HEPES buffer at pH 7.4 increased by factors of 17 and 43, respectively. In addition, the  $\text{Zn}^{2+}$ –**39** complex is much more thermodynamically and kinetically stable than the  $\text{Zn}^{2+}$  complexes of **37** and **38**.

The main drawback of polyamines as receptors is their protonation at neutral pH which competes with  $\text{Zn}^{2+}$  binding. The alkylation of polyamines lower the amine  $\text{p}K_a$  values, so that protonation would be less likely at neutral pH.

To pursue visible excitation, chemosensors **40** and **41** were designed by the Nagano group with fluorescein as the fluorophore and a tetra-substituted cyclen as the ionophore.<sup>51</sup> Their affinity for  $\text{Zn}^{2+}$  was reduced compared with **37**. As expected,

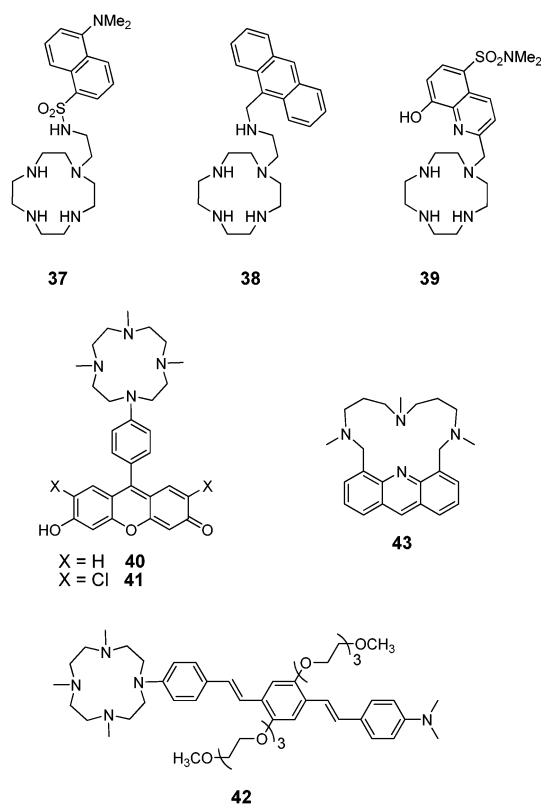


Fig. 15 Structures of chemosensors **37**–**43**.

the fluorescence of **40** and **41** was quenched at pH 7.5 due to PET. Upon addition of 1 equiv. of  $\text{Zn}^{2+}$ , the fluorescence emission intensity of **40** and **41** increased up to 14- and 26-fold, respectively, with no significant change in the position of excitation and emission maxima (for **40**,  $\lambda_{\text{ex}} = 495$  nm;  $\lambda_{\text{em}} = 515$  nm; for **41**,  $\lambda_{\text{ex}} = 505$  nm;  $\lambda_{\text{em}} = 525$  nm). The detection limit of **40** and **41** is 500 nM of  $\text{Zn}^{2+}$  under these conditions, with a signal-to-noise ratio of 3.0.

Recently, Ferrante *et al.* introduced the tetramethylcyclen moiety into a distyrylbenzene structure which has a high two-photon absorption (TPA) cross-section and a noticeable fluorescence quantum yield (compound **42**, Fig. 15).<sup>52</sup> The TPA properties of **42** in DMSO was investigated by the TPA fluorescence excitation technique, in the 720–850 nm wavelength range. The maximum contrast is attained at 750 nm, where a factor of 5 is reached, with the free ligand **42** being more fluorescent than the zinc complex.

Yoon *et al.* reported a new acridine derivative, in which an azacrown ligand is immobilized on the 4 and 5 positions of acridine.<sup>53</sup> Probe **43** displayed a selective fluorescent enhancement effect with  $\text{Zn}^{2+}$  in 100% aqueous solution. The importance of the central nitrogen on the acridine upon binding with  $\text{Zn}^{2+}$  was demonstrated by a control compound; a similar anthracene derivative bearing the same ligand on its 1 and 8 positions, did not display any significant change with the metal ions examined.

## 7. Iminodiacetic acid as the receptor

Iminodiacetic acid and derivatives such as ethylene glycol-bis(2-aminoethylether)-*N,N,N',N'*-tetraacetic acid (EGTA) and bis(*o*-aminophenoxy) ethane-*N,N,N',N'*-tetraacetic acid (BAPTA) were first used to construct fluorescent chemosensors for  $\text{Ca}^{2+}$  and  $\text{Mg}^{2+}$ . In principle,  $\text{Zn}^{2+}$  concentrations can be measured using fluorescent chemosensors nominally designed for  $\text{Ca}^{2+}$  and/or  $\text{Mg}^{2+}$  detection,<sup>54</sup> since most  $\text{Ca}^{2+}$  chemosensors have a higher affinity for  $\text{Zn}^{2+}$  than for  $\text{Ca}^{2+}$ . However, with these probes, the presence of  $\text{Ca}^{2+}$  or  $\text{Mg}^{2+}$  in the sample may interfere with accurate  $\text{Zn}^{2+}$  quantitation. In order to achieve a higher selectivity for  $\text{Zn}^{2+}$  over  $\text{Ca}^{2+}$  or  $\text{Mg}^{2+}$ , Gee *et al.* modified the chelating BAPTA-portion of fluorescent  $\text{Ca}^{2+}$  chemosensors by removing one or more of the chelating moieties to design a series of chemosensors (**44**–**51**, Fig. 16) selective for  $\text{Zn}^{2+}$  with affinities from nanomolar to micromolar and wavelengths from UV to the far red.<sup>55–57</sup> **44** and **45** are ratiometric fluorescent chemosensors for  $\text{Zn}^{2+}$ . With the addition of  $\text{Zn}^{2+}$ , **44** exhibits a fluorescence excitation wavelength shift from 378 nm to 330 nm, and **45** shows a fluorescence wavelength shift from 480 nm to 395 nm. **46**–**51** are PET type chemosensors with fluorescein and rhodamine as fluorophores. Upon zinc binding, **46** undergoes a 200-fold fluorescence increase, which occurs at  $\sim 100$   $\mu\text{M}$   $\text{Zn}^{2+}$ . **50** shows the highest selectivity and affinity for zinc ions ( $\sim 100$  nM  $\text{Zn}^{2+}$ ), while calcium complexation does not result in a detectable response. **47** and **48** exhibit 100- to 150-fold fluorescence increases in the same type of experiment, while **49** only shows a 12-fold fluorescence increase upon  $\text{Zn}^{2+}$  saturation. **51** shows a 75-fold fluorescence increase with the addition of  $\text{Zn}^{2+}$ . Experiments in

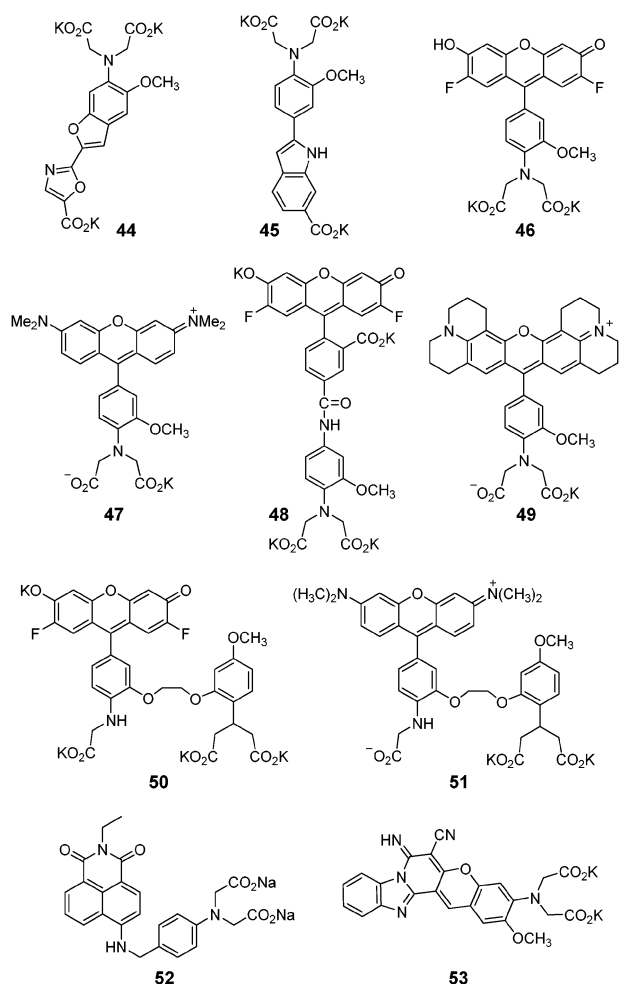


Fig. 16 Structures of chemosensors 44–53.

neuronal cell cultures show that **51** effectively localizes into mitochondria and detects changes of intramitochondrial free  $Zn^{2+}$ .<sup>56</sup>

Gunnlaugsson *et al.* developed a naphthalimide based chemosensor **52** for  $Zn^{2+}$ .<sup>58</sup> A simple aromatic iminodiacetate was selected as the receptor, which is pH independent in the physiological pH range ( $pK_{a1}$  of **52** is 3.1) and offers good water solubility. In addition, the bidentate receptor in **52** adopts a half of the BAPTA structure and shows quite weak affinities for  $Ca^{2+}$  and  $Mg^{2+}$ . **52** displays a 53-fold fluorescence increase with the titration of  $Zn^{2+}$  ( $\lambda_{ex} = 442$  nm;  $\lambda_{em} = 550$  nm;  $K_d = 80$  nM). The competitive analysis revealed that **52** has a high selectivity for  $Zn^{2+}$  over  $Cu^{2+}$ ,  $Cd^{2+}$  and  $Hg^{2+}$ , as well as  $Ca^{2+}$  and  $Mg^{2+}$ . Recently, Katerinopoulos *et al.* reported a red emitting ratiometric fluorescent chemosensor **53** with nanomolar affinity ( $K_d = 4$  nM) for zinc ions using the chromeno[3',2':3,4]pyrido[1,2a][1,3]benzimidazole moiety as the fluorophore.<sup>59</sup> The  $Zn^{2+}$ -binding induces 26 nm shift in emission of **53** from 590 nm to 564 nm associated with the shift in excitation spectra from 553 nm to 543 nm.

Iminodiacetic acid based receptors usually have nanomolar affinity for zinc ions and good water solubility. But the main drawback of this type receptor is the fluorescence interference by  $Ca^{2+}$  binding. These probes are therefore unsuitable for biological applications.

## 8. Triazole as the receptor

In 2001, Sharpless *et al.* introduced the chemical philosophy of 'Click chemistry'.<sup>60</sup> The foundation of 'click chemistry' is termed by generation of chemical substances by joining small units together through a convenient reaction in high chemical yield and selectivity in a wide range of substrates.<sup>61</sup> The most popular click reaction of click chemistry is the copper(I)-catalysed 1,2,3-triazole forming reaction between azides and terminal alkynes due to its reliability, specificity and bio-compatibility. With respect to a chemosensor, the triazole formed during this click reaction can act as a ligand for metal ions. Moreover, the advantage of the triazole as a metal receptor is that the click reaction can efficiently and conveniently connect the fluorophore and the receptor in a favorable geometry. This also indicates that the triazole should combine with other binding sites like DPA or polyamine to act as receptor for zinc ion.

Yang and co-workers used triazole as a spacer to connect two pyrenes to the lower rims of calix[4]arene (compound **54**, Fig. 17).<sup>62</sup> The  $Zn^{2+}$ -free form of **54** displays a strong pyrene excimer emission at 482 nm when excited at 343 nm in  $CH_3CN$ . The addition of  $Zn^{2+}$  caused an increase in the monomer emission, and a concomitant decrease in the excimer emission. But **54** also has strong affinities for other transition ions. The addition of  $Cu^{2+}$ ,  $Hg^{2+}$ , or  $Pb^{2+}$  caused a remarkable decrease of fluorescence intensities of both the excimer and monomer. Recently, Leroux and co-workers synthesized a tridentate [1,2,3]triazolo[1,5-a]pyridine derivative **55** as a chemosensor for zinc ions, nitrite and cyanide anions.<sup>63</sup> The addition of  $Zn^{2+}$  to **55** leads to very significant enhancement of fluorescence accompanied by a small hypsochromic effect. The addition of nitrite or cyanide anion to **55**/ $Zn^{2+}$  1 : 1 solution quenches the fluorescence. Zhu *et al.* connected DPA to anthracene through a triazole to produce compound **56**, in which DPA and the triazole cooperate as a tetradentate ligand for  $Zn^{2+}$ .<sup>64</sup> The  $Zn^{2+}$  binding causes a 7.8-fold enhancement in the emission of **56** in water ( $\lambda_{ex} = 300$  nm;  $\lambda_{em} = 462$  nm;  $K_d = 12$  nM). Watkinson and co-workers recently reported chemosensor **57**, in which a cyclam (1,4,8,11-tetraazacyclotetradecane) based macrocyclic receptor is linked to a naphthalimide fluorophore by using a click reaction.<sup>65</sup> The triazole acts as a scorpionate ligand on the cyclam macrocycle. A 6-fold enhancement of fluorescence emission up to the

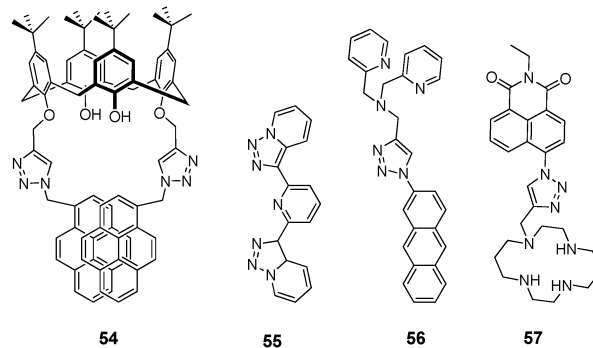


Fig. 17 Structures of chemosensors 54–57.

addition of 1 equiv. of zinc ion is consistent with the formation of 1 : 1 complex ( $\lambda_{\text{ex}} = 350 \text{ nm}$ ;  $\lambda_{\text{em}} = 407 \text{ nm}$ ;  $K_{\text{d}} = 43 \text{ nM}$ ).

## 9. Schiff-base as the receptor

The nitrogen of a Schiff base also exhibits a strong affinity for zinc. Therefore the Schiff base has also been used to develop zinc chemosensors. The C=N isomerization is the predominant decay process of the excited states for compounds with an unbridged C=N structure so that those compounds are often nonfluorescent. In contrast, the fluorescence of its analogues with a covalently bridged C=N structure increases dramatically due to the suppression of C=N isomerization in the excited states.<sup>66</sup> Therefore the C=N isomerization can be applied in the design of chemosensors for metal ions. The binding of metal ions by the C=N group would stop the isomerization, and a significant fluorescence enhancement could be achieved. Following this strategy, Wang *et al.* designed a coumarin derivative **58** (Fig. 18).<sup>67</sup> The free ligand **58** is almost nonfluorescent due to the isomerization of the C=N double bond in the excited state. However, the CH<sub>3</sub>CN solution of **58** shows about a 200-fold increase of fluorescence quantum yield upon addition of zinc ions associated with a red-shift in emission from 500 to 522 nm ( $\lambda_{\text{ex}} = 450 \text{ nm}$ ).

Yoon *et al.* recently reported a simple and effective fluorescent sensor (**59**) based on the hydrazone-pyrene.<sup>68</sup> This probe displays a highly selective fluorescent enhancement with Zn<sup>2+</sup>, and application of this probe to detect the intrinsic Zn<sup>2+</sup> ions present in pancreatic cells was successfully demonstrated. The absence of any significant change in absorption spectra upon the addition of Zn<sup>2+</sup> indicates that large fluorescence

enhancement with Zn<sup>2+</sup> can be attributed to the blocking of the PET process from nitrogen in the hydrazone moiety to pyrene. The authors successfully demonstrated that probe **59** could monitor the level of intrinsic Zn<sup>2+</sup> in pancreatic cells.

The appeal of C=N based fluorescent chemosensors is the large fluorescence enhancement induced by metal ion chelation. Compounds **60–65** all apply the C=N isomerization to act as zinc chemosensors with turn-on fluorescence signals.<sup>69–74</sup> However, the main drawbacks of Schiff-base type receptors are the poor solubility and the instability of the Schiff-base in aqueous solutions. Except for compound **61**, the optical properties of **60–65** were all detected in CH<sub>3</sub>CN solutions. In addition, such a simple receptor cannot show good binding-selectivity for zinc ions. But it can be a promising binding site to assembly with other Zn<sup>2+</sup> receptors.

## 10. Concluding remarks

In this review, we cover Zn<sup>2+</sup> probes using the classification of receptor types. There has been tremendous interest in detecting Zn<sup>2+</sup> due to its special biological importance; therefore, many receptors have been reported connected to various fluorophores. However, there is still much scope to improve the receptors for zinc to satisfy criteria such as fast chelation, high sensitivity/selectivity, high bio-compatibility, and fluorescence bio-imaging capacity. Accordingly, the design of the zinc receptor in the probe is the most important issue. Most of the known receptors use nitrogen as the coordination site and the geometries of receptors are relatively simple. To fulfil the myriad criteria, diversity should be concerned in the design of receptors in the future. The diversity should at least include two aspects. One is the diverse binding sites and geometry of the receptors. For example, in compound **22**, the Schiff-base nitrogen cooperates with DPA as the receptor, while in compound **56** the triazole cooperates with DPA. Another aspect of diversity is the diverse coordination approaches with similar guests. The ‘receptor transformation’ strategy of **22** is a good example.

## Acknowledgements

We gratefully acknowledge financial support from the EPSRC, BBSRC, MRC, Newman Trust, Herchel Smith Fellowship Fund, the National Research Foundation of Korea (NRF) (20090083065, 20090063001), the WCU program (R31-2008-000-10010-0), and State Key Laboratory of Fine Chemicals of China (KF0809).

## Notes and references

- R. Y. Tsien, in *Fluorescent and Photochemical Probes of Dynamic Biochemical Signals inside Living Cells*, ed. A. W. Czarnik, American Chemical Society, Washington, DC, 1993, pp. 130–146.
- A. P. de Silva, H. Q. Nimal Gunaratne, T. Gunnlaugsson, A. J. M. Huxley, C. P. McCoy, J. T. Rademacher and T. E. Rice, *Chem. Rev.*, 1997, **97**, 1515.
- C. J. Frederickson, J.-Y. Koh and A. I. Bush, *Nat. Rev. Neurosci.*, 2005, **6**, 449.
- A. I. Bush, W. H. Pettingell, G. Multhaup, M. Paradis, J.-P. Vonsattel, J. F. Gusella, K. Beyreuther, C. L. Masters and R. E. Tanzi, *Science*, 1994, **265**, 1464.

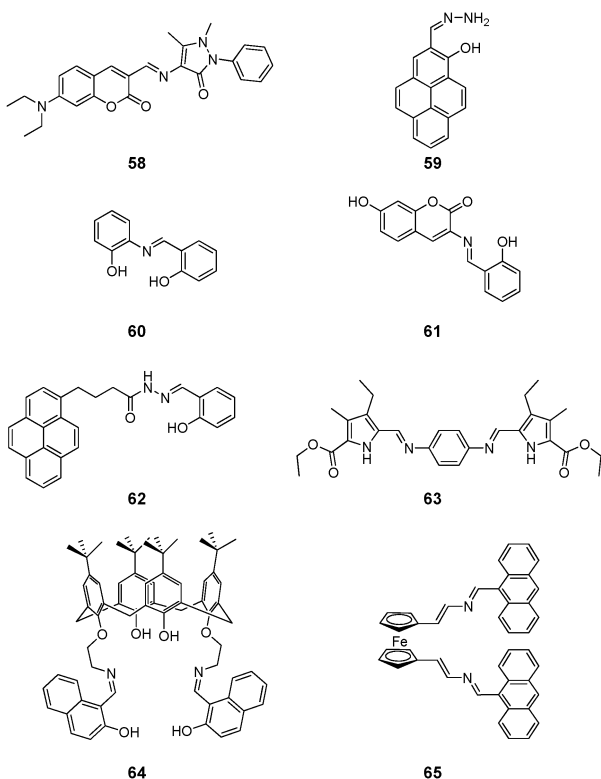


Fig. 18 Structures of chemosensors **58–65**.

- 5 E. L. Que, D. W. Domaille and C. J. Chang, *Chem. Rev.*, 2008, **108**, 1517.
- 6 P. Jiang and J. Guo, *Coord. Chem. Rev.*, 2004, **248**, 205.
- 7 P. Carol, S. Sreejith and A. Ajayaghosh, *Chem.–Asian J.*, 2007, **2**, 338.
- 8 E. Kimura and S. Aoki, *BioMetals*, 2001, **14**, 191.
- 9 R. P. Haugland, *Handbook of Fluorescent Probes and Research Chemicals*, ed. M. T. Z. Spence, Molecular Probes, Eugene, OR, 6th edn, 1996, pp. 530–540.
- 10 S. A. de Silva, A. Zavaleta, D. E. Baron, O. Allam, E. V. Isidor, N. Kashimura and J. M. Percarpio, *Tetrahedron Lett.*, 1997, **38**, 2237.
- 11 S. C. Burdette, G. K. Walkup, B. Spingler, R. Y. Tsien and S. J. Lippard, *J. Am. Chem. Soc.*, 2001, **123**, 7831.
- 12 C. J. Chang, E. M. Nolan, J. Jaworski, S. C. Burdette, M. Sheng and S. J. Lippard, *Chem. Biol.*, 2004, **11**, 203.
- 13 A. Loudet and K. Burgess, *Chem. Rev.*, 2007, **107**, 4891.
- 14 Y. Wu, X. Peng, B. Guo, J. Fan, Z. Zhang, J. Wang, A. Cui and Y. Gao, *Org. Biomol. Chem.*, 2005, **3**, 1387.
- 15 S. Atilgan, T. Ozdemir and E. U. Akkaya, *Org. Lett.*, 2008, **10**, 4065.
- 16 W. Jiang, Q. Fu, H. Fan and W. Wang, *Chem. Commun.*, 2008, 259.
- 17 C. L. Amiot, S. Xu, S. Liang, L. Pan and J. X. Zhao, *Sensors*, 2008, **8**, 3082.
- 18 B. Tang, H. Huang, K. Xu, L. Tong, G. Yang, X. Liu and L. An, *Chem. Commun.*, 2006, 3609.
- 19 E. Kawabata, K. Kikuchi, Y. Urano, H. Kojima, A. Odani and T. Nagano, *J. Am. Chem. Soc.*, 2005, **127**, 818.
- 20 T. Hirano, K. Kikuchi, Y. Urano, T. Higuchi and T. Nagano, *J. Am. Chem. Soc.*, 2000, **122**, 12399.
- 21 S. Maruyama, K. Kikuchi, T. Hirano, Y. Urano and T. Nagano, *J. Am. Chem. Soc.*, 2002, **124**, 10650.
- 22 K. Kiyose, H. Kojima, Y. Urano and T. Nagano, *J. Am. Chem. Soc.*, 2006, **128**, 6548.
- 23 J. Wang, Y. Xiao, Z. Zhang, X. Qian, Y. Yang and Q. Xu, *J. Mater. Chem.*, 2005, **15**, 2836.
- 24 Z. Xu, X. Qian, J. Cui and R. Zhang, *Tetrahedron*, 2006, **62**, 10117.
- 25 C. Lu, Z. Xu, J. Cui, R. Zhang and X. Qian, *J. Org. Chem.*, 2007, **72**, 3554.
- 26 Z. Xu, G. Kim, S. Han, M. Jou, C. Lee, I. Shin and J. Yoon, *Tetrahedron*, 2009, **65**, 2307.
- 27 F. Qian, C. Zhang, Y. Zhang, W. He, X. Gao, P. Hu and Z. Guo, *J. Am. Chem. Soc.*, 2009, **131**, 1460.
- 28 Z. Liu, C. Zhang, Y. Li, Z. Wu, F. Qian, X. Yang, W. He, X. Gao and Z. Guo, *Org. Lett.*, 2009, **11**, 795.
- 29 M. Taki, J. L. Wolford and T. V. O'Halloran, *J. Am. Chem. Soc.*, 2004, **126**, 712.
- 30 K. Komatsu, Y. Urano, H. Kojima and T. Nagano, *J. Am. Chem. Soc.*, 2007, **129**, 13447.
- 31 Z. Xu, K. Baek, H. Kim, J. Cui, X. Qian, D. R. Spring, I. Shin and J. Yoon, *J. Am. Chem. Soc.*, 2010, **132**, 601.
- 32 E. M. Nolan, J. W. Ryu, J. Jaworski, R. P. Feazell, M. Sheng and S. J. Lippard, *J. Am. Chem. Soc.*, 2006, **128**, 15517.
- 33 K. Komatsu, K. Kikuchi, H. Kojima, Y. Urano and T. Nagano, *J. Am. Chem. Soc.*, 2005, **127**, 10197.
- 34 C. J. Frederickson, E. J. Kasarskis, D. Ringo and R. E. Frederickson, *J. Neurosci. Methods*, 1987, **20**, 91.
- 35 P. D. Zalewski, S. H. Millard, I. J. Forbes, O. Kapaniris, A. Slavotinek, W. H. Betts, A. D. Ward, S. F. Lincoln and I. Mahadevan, *J. Histochem. Cytochem.*, 1994, **42**, 877.
- 36 Y. Zhang, X. Guo, W. Si, L. Jia and X. Qian, *Org. Lett.*, 2008, **10**, 473.
- 37 H. Wang, Q. Gan, X. Wang, L. Xue, S. Liu and H. Jiang, *Org. Lett.*, 2007, **9**, 4995.
- 38 E. M. Nolan, J. Jaworski, K.-I. Okamoto, Y. Hayashi, M. Sheng and S. J. Lippard, *J. Am. Chem. Soc.*, 2005, **127**, 16812.
- 39 W.-S. Xia, R. H. Schmehl and C.-J. Li, *J. Am. Chem. Soc.*, 1999, **121**, 5599.
- 40 J. V. Mello and N. S. Finney, *Angew. Chem., Int. Ed.*, 2001, **40**, 1536.
- 41 A. Ajayaghosh, P. Carol and S. Sreejith, *J. Am. Chem. Soc.*, 2005, **127**, 14962.
- 42 A. E. Dennis and R. C. Smith, *Chem. Commun.*, 2007, 4641.
- 43 L. Zhang, R. J. Clark and L. Zhu, *Chem.–Eur. J.*, 2008, **14**, 2894.
- 44 M. E. Huston, K. W. Haider and A. W. Czarnik, *J. Am. Chem. Soc.*, 1988, **110**, 4460.
- 45 J. A. Sclafani, M. T. Maranto, T. M. Sisk and S. A. Van Arman, *Tetrahedron Lett.*, 1996, **37**, 2193.
- 46 L. Prodi, F. Bolletta, M. Montalti and N. Zaccheroni, *Eur. J. Inorg. Chem.*, 1999, 455.
- 47 T. Koike, T. Watanabe, S. Aoki, E. Kimura and M. Shiro, *J. Am. Chem. Soc.*, 1996, **118**, 12696.
- 48 E. Kimura, S. Aoki, E. Kikuta and T. Koike, *Proc. Natl. Acad. Sci. U. S. A.*, 2003, **100**, 3731.
- 49 S. Aoki, S. Kaido, H. Fujioka and E. Kimura, *Inorg. Chem.*, 2003, **42**, 1023.
- 50 S. Aoki, K. Sakurama, N. Matsuo, Y. Yamada, R. Takasawa, S. Tanuma, M. Shiro, K. Takeda and E. Kimura, *Chem.–Eur. J.*, 2006, **12**, 9066.
- 51 T. Hirano, K. Kikuchi, Y. Urano, T. Higuchi and T. Nagano, *Angew. Chem., Int. Ed.*, 2000, **39**, 1052.
- 52 R. Bozio, E. Cecchetto, G. Fabbri, C. Ferrante, M. Maggini, E. Menna, D. Pedron, R. Riccò, R. Signorini and M. Zerbetto, *J. Phys. Chem. A*, 2006, **110**, 6459.
- 53 M. S. Park, K. M. K. Swamy, Y. J. Lee, H. N. Lee, Y. J. Jang, Y. H. Moon and J. Yoon, *Tetrahedron Lett.*, 2006, **47**, 8129.
- 54 L. M. Canzoniero, S. L. Sensi and D. W. Choi, *Neurobiol. Dis.*, 1997, **4**, 275.
- 55 K. R. Gee, Z.-L. Zhou, D. Ton-That, S. L. Sensi and J. H. Weiss, *Cell Calcium*, 2002, **31**, 245.
- 56 S. L. Sensi, D. Ton-That, J. H. Weiss, A. Rothe and K. R. Gee, *Cell Calcium*, 2003, **34**, 281.
- 57 K. R. Gee, Z.-L. Zhou, W.-J. Qian and R. Kennedy, *J. Am. Chem. Soc.*, 2002, **124**, 776.
- 58 T. Gunnlaugsson, T. Clive Lee and R. Parkesh, *Org. Biomol. Chem.*, 2003, **1**, 3265.
- 59 E. Roussakis, S. Voutsadaki, E. Pinakoulaki, D. P. Sideris, K. Tokatlidis and H. E. Katerinopoulos, *Cell Calcium*, 2008, **44**, 270.
- 60 H. C. Kolb, M. G. Finn and K. B. Sharpless, *Angew. Chem., Int. Ed.*, 2001, **40**, 2004.
- 61 J. E. Moses and A. D. Moorhouse, *Chem. Soc. Rev.*, 2007, **36**, 1249.
- 62 L. Zhu, S. Gong, S. Gong, C. Yang and J. Qin, *Chin. J. Chem.*, 2008, **26**, 1424.
- 63 R. Ballesteros-Garrido, B. Abarca, R. Ballesteros, C. R. de Arellano, F. R. Leroux, F. Colobert and E. García-España, *New J. Chem.*, 2009, **33**, 2102.
- 64 S. Huang, R. J. Clark and L. Zhu, *Org. Lett.*, 2007, **9**, 4999.
- 65 E. Tamanini, A. Katewa, L. M. Sedger, M. H. Todd and M. Watkinson, *Inorg. Chem.*, 2009, **48**, 319.
- 66 G. Q. Yang, F. Morlet-Savary, Z. K. Peng, S. K. Wu and J. P. Fouassier, *Chem. Phys. Lett.*, 1996, **256**, 536.
- 67 J. Wu, W. Liu, X. Zhuang, F. Wang, P. Wang, S. Tao, X. Zhang, S. Wu and S. Lee, *Org. Lett.*, 2007, **9**, 33.
- 68 Y. Zhou, H. N. Kim and J. Yoon, *Bioorg. Med. Chem. Lett.*, 2010, **20**, 125.
- 69 N. Xie and Y. Chen, *Chin. J. Chem.*, 2006, **24**, 1800.
- 70 H. Li, S. Gao and Z. Xi, *Inorg. Chem. Commun.*, 2009, **12**, 300.
- 71 N. Li, Y. Xiang, X. Chen and A. Tong, *Talanta*, 2009, **79**, 327.
- 72 Z. Wu, Y. Zhang, J. S. Ma and G. Yang, *Inorg. Chem.*, 2006, **45**, 3140.
- 73 J. Dessingou, R. Joseph and C. R. Rao, *Tetrahedron Lett.*, 2005, **46**, 7967.
- 74 F. Zapata, A. Caballero, A. Espinosa, A. Tarraga and P. Molina, *Org. Lett.*, 2007, **9**, 2385.